

Figure 1: Illustration of the barcodes based on a sequence of Rips complexes for a point cloud.

- 1 Fig. 1 depicts an example of barcode representations (including 0-, 1-, and 2-dimensional topological  
 2 features, i.e.,  $H_0$ ,  $H_1$ , and  $H_2$ ) of homology over a point cloud. We observe that, by gradually  
 3 changing the threshold  $\epsilon$ , the barcode representation can filter out topological noises, and capture  
 4 significant topological and higher-order features.
- 5 In brief, the key idea here is to choose some suitable scale parameters  $\epsilon$  to study changes in homology  
 6 that occur to  $x$  which evolves with respect to  $\epsilon$ . That is, we no longer treat  $x$  as a single object but  
 7 as a filtration  $x_{\epsilon_1} \subseteq \dots \subseteq x_{\epsilon_n} = x$ , induced by monotonic changes of  $\epsilon$ . To make the process of  
 8 pattern counting more systematic and efficient, we build an abstract simplicial complex  $\mathcal{K}(x_{\alpha_j})$  on  
 9 each  $x_{\alpha_j}$ , resulting in a filtration of complexes  $\mathcal{K}(x_{\epsilon_1}) \subseteq \dots \subseteq \mathcal{K}(x_{\epsilon_n})$ . For instance, we can  
 10 select a scale parameter as a distance (e.g., edge weight) between any two points; then generate an  
 11 abstract simplicial complex  $\mathcal{K}(x_{\epsilon_*})$  by producing sub-point clouds  $x'$  with a bounded diameter  $\epsilon_*$   
 12 (i.e.,  $(k-1)$ -simplex in  $\mathcal{K}(x_{\epsilon_*})$  is made up by sub-point clouds  $x'$  of  $k$ -nodes with  $\text{diam}(x') \leq \epsilon_*$ ).
- 13 As shown in Fig. 2, we randomly sampled 64 images from (a) CREMI dataset; (b) Topo-Diffusion  
 14 model, (c) DDPM, (d) Topo-GAN, and (e) WGAN. We sampled the CREMI dataset into sizes of  
 15  $64 \times 64$ . The visualization shows that a diffusion based model outperformed a GAN based model in  
 16 the diversity phase. Furthermore, topological aware methods (i.e., Topodiffusion and TopoGAN) can  
 17 capture more topological mode of the original dataset. From qualitative visualizations, we can see  
 18 that the image quality as well as diversity can be improved from the TopoDiffusion model.
- 19 We train our Topo-Diffusion model with a pretraining network. We set all vectorized topological  
 20 summaries as identity vectors in the pertraining and pretrain the Topo-Diffusion model for 100k  
 21 steps. After pretraining, we train all of the models (including baseline or DDPM, Topo-Diffusion  
 22 with persistence landscape, Topo-Diffusion with betti curves, Topo-Diffusion with persistence image)  
 23 for 1 million steps (Figs. 3-5).

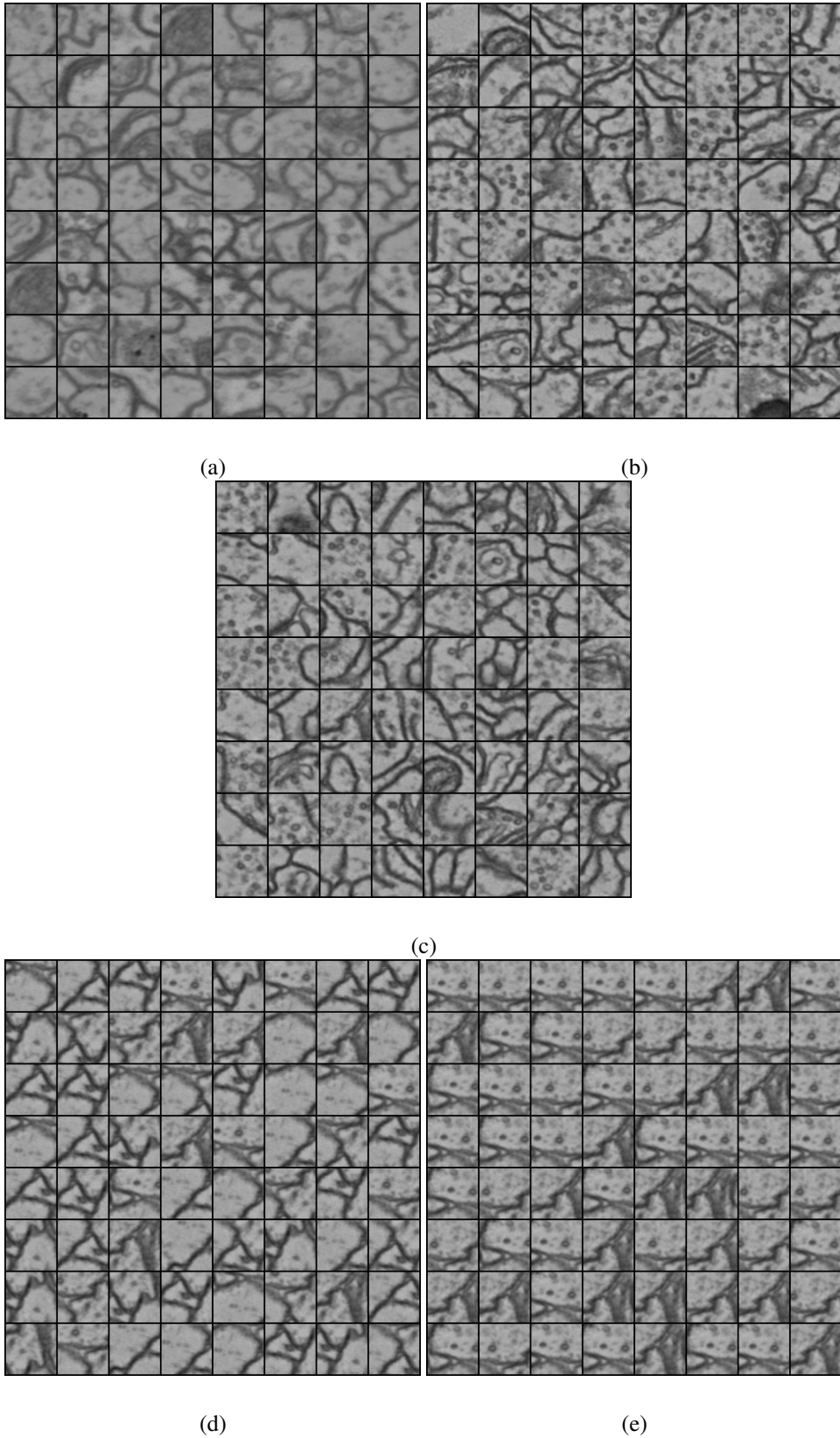


Figure 2: Visualization of (a) Training data, and generated CREMI images from (b) Topo-Diffusion model,(c) DDPM, (d) Topo-GAN, and (e) WGAN.

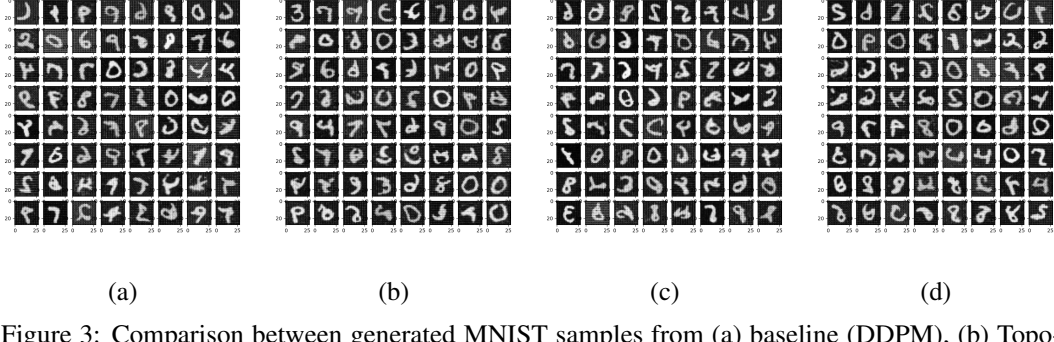


Figure 3: Comparison between generated MNIST samples from (a) baseline (DDPM), (b) Topo-Diffusion based on persistence landscape, (c) Topo-Diffusion based on Betti curve, and (d) Topo-Diffusion based on persistence image.

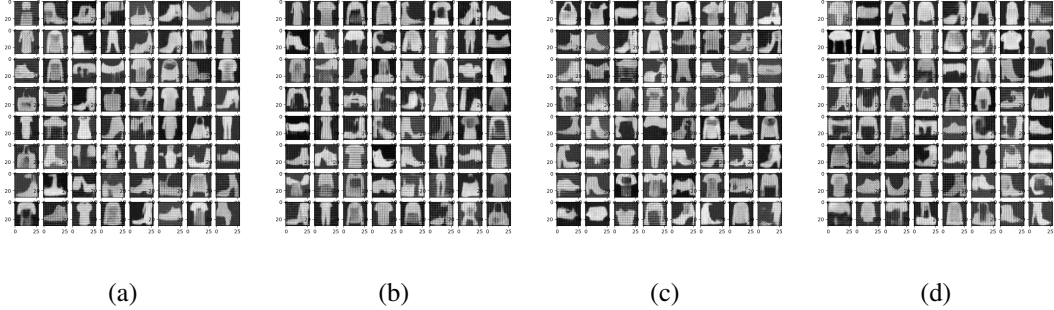


Figure 4: Comparison between generated Fashion MNIST samples from (a) baseline (DDPM), (b) Topo-Diffusion based on persistence landscape, (c) Topo-Diffusion based on Betti curve, and (d) Topo-Diffusion based on persistence image.

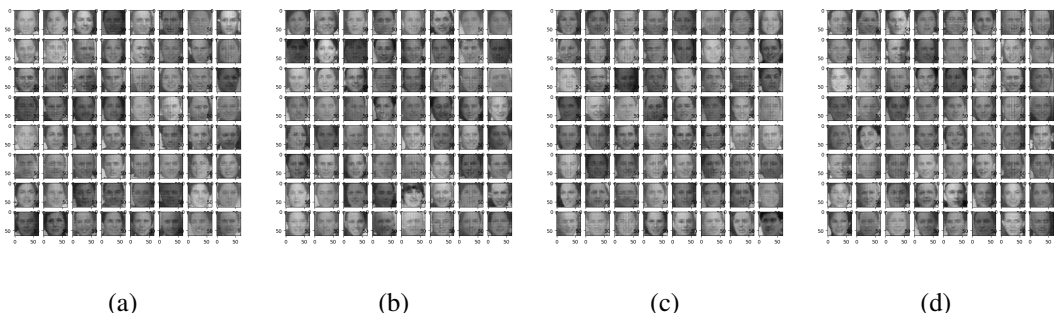


Figure 5: Comparison between generated LFW samples from (a) baseline (DDPM), (b) Topo-Diffusion based on persistence landscape, (c) Topo-Diffusion based on Betti curve, and (d) Topo-Diffusion based on persistence image.